

## Influence of heat treatment on microwave dielectric properties of erbium doped borotellurite glass ceramics

S. Othman <sup>a</sup>, Y. H. Lua <sup>b</sup>, E. S. Sazali <sup>a\*</sup>, Y. S. Yap <sup>b\*</sup>, R. Hisam <sup>c</sup>

<sup>a</sup> *Advanced Optical Materials Research Group, Department of Physics, Faculty of Science, Universiti Teknologi Malaysia, Skudai, Johor 81310, Malaysia*

<sup>b</sup> *Faculty of Science and Centre for Sustainable Nanomaterials (CsNano), Universiti Teknologi Malaysia, Skudai, Johor 81310, Malaysia*

<sup>c</sup> *Faculty of Applied Sciences, Universiti Teknologi MARA, 40450, Shah Alam, Selangor, Malaysia*

High-performance glass-ceramics are increasingly explored for their suitability in high-frequency dielectric applications, presenting a significant challenge in materials science. A primary focus has been allocated to investigating borotellurite glasses operating at frequencies below 15 MHz. Borotellurite glasses with the composition 69TeO<sub>2</sub>-10B<sub>2</sub>O<sub>3</sub>-10PbO-10ZnO-1Er<sub>2</sub>O<sub>3</sub> were fabricated via the melt-quenching method. This study examines the effects of heat treatment durations (1–24 hours) on these glasses. Variations in density, molar volume, structure, and dielectric properties were attributed to changes in non-bridging oxygen bonding resulting from the heat treatments. X-ray diffraction analysis confirmed the amorphous nature of the as-quenched glass. Morphological changes due to heat treatment were analyzed using field emission scanning electron microscopy, revealing grain size variations between 0.237 and 1.509 μm. Dielectric constant and loss tangent were measured at approximately 7 GHz using a resonant method for both glass and glass-ceramic phases at different crystallization times. Heat treatment increased the crystalline volume fraction within the glass-ceramic. The resulting material demonstrated a dielectric constant up to 17.75 ± 9 % and a dielectric loss of 1.03 × 10<sup>-4</sup> ± 17 %, indicating potential for use in microwave applications.

(Received November 27, 2024; Accepted May 5, 2025)

**Keywords:** Borotellurite glass, Dielectric constant, Dielectric loss

### 1. Introduction

Microwave frequencies, a critical part of the electromagnetic spectrum, have become indispensable due to their diverse applications in modern technology. One compelling avenue of exploration lies in utilizing glass ceramics as substrates for microwave technologies. Dielectric materials are integral to microwave technologies, valued for their interaction with electric fields and their frequency-specific dielectric constants and losses. Glass ceramics have recently gained popularity due to their optimal dielectric constants and low dielectric losses. To be more specific, borotellurite glass ceramic is intriguing, however it is often investigated at frequencies lower than 15 MHz [1, 2, 3, 4]. Recent technological developments have expanded applications to higher frequencies, surpassing the 1 GHz threshold.

Borotellurite glasses stand out as particularly attractive among tellurite materials. These glasses exhibit a high refractive index, wide transparency window, and good glass-forming ability, making them suitable for fiber optic and amplifier applications [5]. They have also been extensively studied for their gamma radiation shielding capabilities, owing to their minimal changes in structural and optical properties under irradiation as reported most recently by Patra [6]. This glass is also used in microelectronics applications. In addition, incorporating modifiers like zinc oxide helps lower the melting temperature and provides high polarizability, which is essential for improving the dielectric properties [7]. Furthermore, addition of lead oxides which also act as the modifier are useful in

---

\* Corresponding authors: ezzasyuhada@utm.my  
<https://doi.org/10.15251/CL.2025.225.451>

photovoltaic materials with high carrier mobilities, conductivities and strong absorption cross sections [7]. Because rare earth (RE) ions have outstanding optoelectronic properties and are easy to fabricate, it is very desired to include them into doped glasses [8]. Adding erbium to borotellurite glass improves its usefulness for microwave applications. Erbium doping leads to better light emission, stronger optical signals, and control over the material's interaction with specific wavelengths [5]. The development of rare-earth glasses has already involved crystallization through controlled heat treatments. Kinetic and thermodynamic variables play a major role in the nucleation and growth processes that lead to crystallization [9]. Annealing temperatures exceeding the glass transition temperature can affect both nucleation and crystal growth processes [9]. The crystallization process, driven by nucleation and growth, is strongly affected by kinetic and thermodynamic factors. Notably, annealing above the glass transition temperature can control both nucleation and growth. This study explores how varying heat treatment durations influence the nucleation and growth of nanoparticles, leading to changes in the spectroscopic properties of erbium-doped borotellurite. Furthermore, the study investigates the enhancement of dielectric properties due to heat treatment.

## 2. Experimental details

Glasses with the composition  $69\text{TeO}_2\text{-}10\text{B}_2\text{O}_3\text{-}10\text{PbO-}10\text{ZnO-}1\text{Er}_2\text{O}_3$  were synthesized using a melt-quenching method. The starting materials were thoroughly mixed by repeated grinding. The mixture was then melted in an alumina crucible at  $1000^\circ\text{C}$  for 30 minutes under atmospheric conditions to ensure homogeneity. The molten glass was rapidly quenched by casting into a 2 mm diameter rod mold at room temperature. To facilitate crystallization, heat treatments were performed at  $399^\circ\text{C}$  for varying durations of 1, 6, 16, and 24 hours. After heat treatment, samples were rapidly cooled to room temperature. Details of the as quenched and heat-treated samples are provided in Table 1.

*Table 1. Borotellurite glass composition in mol% varying heat treatment time (HT).*

Sample	$\text{B}_2\text{O}_3$	$\text{TeO}_2$	$\text{PbO}$	$\text{ZnO}$	$\text{Er}_2\text{O}_3$	HT (hour)
BTPZE	10	69.0	10	10	1.0	-
BTPZE-1	10	69.0	10	10	1.0	1
BTPZE-6	10	69.0	10	10	1.0	6
BTPZE-16	10	69.0	10	10	1.0	16
BTPZE-24	10	69.0	10	10	1.0	24

An analytical balance (Precisa XT220A) was used to measure the glass density via the Archimedes method, with toluene serving as the immersion liquid. The glass density was determined using the Archimedes principle and calculated with the corresponding equation:

$$\rho = \frac{w_a}{w_a - w_l}(\rho_l - \rho_a) + \rho_a \quad (1)$$

X-ray diffraction (XRD) (Model-Siemens Diffractometer D5000) and field emission scanning electron microscopy (FE-SEM; Model JEM-2100F JEOL) were used to investigate the phase evolution and the microstructure of the glass-ceramic samples. The dielectric behaviors at a microwave frequency (range of 7–8 GHz) were measured using the  $\text{TE}_{101}$  mode of standard resonant rectangular cavity with a network analyzer (SA124B) for  $S_{21}$  measurement. In this method, the rod-shaped glass-ceramic sample (2mm diameter) was positioned in the region of the cavity with the highest electric field strength. The cavity's resonant frequency and quality factor (Q) were measured both when empty and with the sample present. Weak coupling, achieved using a small circular

aperture, was employed to maximize the Q factor. The real and imaginary components of the relative permittivity were then calculated from these measured values using the following formula [10]:

$$\varepsilon' = \frac{V_c(f_c - f_s)}{2V_s f_s} + 1 \quad (2)$$

$$\varepsilon'' = \left( \frac{\varepsilon' - 1}{2\varepsilon'} \right) \frac{f_s}{f_c - f_s} \left( \frac{1}{Q_s} - \frac{1}{Q_c} \right) \quad (3)$$

$$\tan \delta = \frac{\varepsilon''}{\varepsilon'} \quad (4)$$

where  $Q_c$  and  $Q_s$  are the quality factors of the cavity without and with the sample present, respectively,  $V_c$  and  $V_s$  denotes the volumes of the cavity and the sample, respectively while  $f_c$  and  $f_s$  are the resonant frequencies without and with sample, respectively.

### 3. Results and discussion

#### 3.1. XRD analysis

Figure 1 displays the typical XRD patterns for glass of BTPZE as a function of the  $2\theta$  scale. The amorphous nature of the BTPZE glass sample is confirmed by the presence of a broad peak between  $25^\circ$  and  $30^\circ$  in the diffraction pattern, with no sharp crystalline peaks observed.

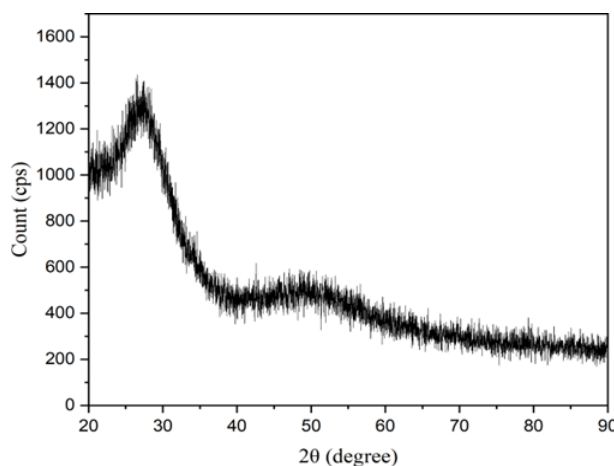


Fig. 1. X-Ray diffraction patterns for BTPZE.

#### 3.2. Physical properties

Figure 2 illustrates the density and molar volume variations for  $69\text{TeO}_2\text{--}10\text{B}_2\text{O}_3\text{--}10\text{PbO--}10\text{ZnO--}1\text{Er}_2\text{O}_3$  glass subjected to different heat treatment durations. It is interesting to note that extended heat treatment times of up to 24 hours increase the production of non-bridging oxygen and raise the density of glass from  $5.45 \text{ g.cm}^{-3}$  to  $14.7 \text{ gcm}^{-3}$  [9]. Meanwhile, the observed decrease in the molar volume, which goes from  $27.3532\text{--}10.1219 \text{ cm}^3/\text{mol}$  is caused by the decrease in the molar volume that supports the glass compactness [11]. The link length and interatomic distance in the glass network are shrinking as a result of the heat-treatment process. The network stiffness was further improved by the glass structure's abundance of bridging oxygen (BO) [12]. The reduction in molar volume suggests that the loose network in the glass under investigation compressed as a result of the heat treatment procedure.

Table 2. Density and molar volume of erbium doped borotellurite glass ceramics.

Sample	Density (g/cm <sup>3</sup> )	Molar Volume (cm <sup>3</sup> /mol)
BTPZE	5.45 ± 0.03	27.35 ± 0.1
BTPZE-1	4.54 ± 0.03	32.80 ± 0.1
BTPZE-6	6.35 ± 0.02	23.47 ± 0.2
BTPZE-16	6.35 ± 0.02	23.47 ± 0.2
BTPZE-24	14.7 ± 0.03	10.12 ± 0.3

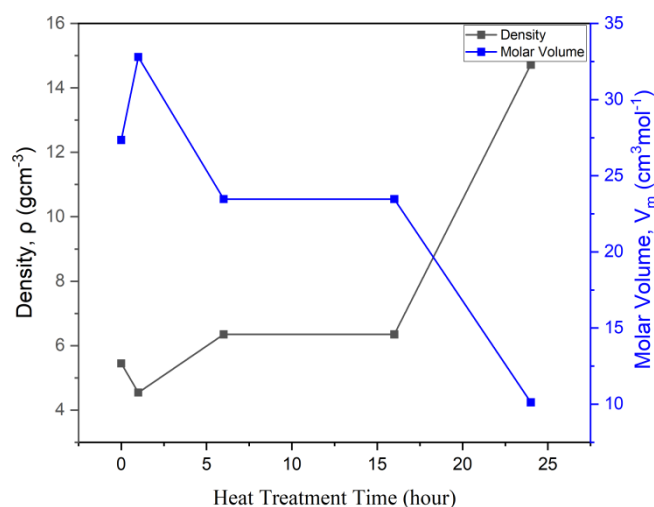


Fig. 2. The heat treatment time dependent of density and molar volume.

### 3.3. FESEM

Figure 3 shows the EDX spectra of 69TeO<sub>2</sub>-10B<sub>2</sub>O<sub>3</sub>-10PbO-10ZnO-1Er<sub>2</sub>O<sub>3</sub>. The EDX analysis confirmed the presence of boron (B), tellurium (Te), zinc (Zn), lead (Pb), erbium (Er) and oxygen (O) elements. Glass-ceramics crystallized at 1,6,16 and 24 h present an average grain size of 0.760  $\mu$ m, 1.051  $\mu$ m, 1.543  $\mu$ m, and 1.509  $\mu$ m, respectively as shown in Figure 4. Figure 5 shows the FESEM micrographs of glass and glass ceramic. The un-treated sample has different morphological structures and grain size compared with the heat-treated sample. The crystal size increases as the crystallization period increases. FESEM examination reveals that longer crystallization time resulted in increased nucleation and grain development during subsequent devitrification. The glass-ceramics have a homogeneous, dense microstructure with uniformly distributed grain sizes and consistent grain shapes. It has been noticed that when the temperature of crystallization rises, the average grain size increases. The development of the nuclei after heat treatment, which happens via the processes of Ostwald ripening and nuclei displacement followed by fusion, is responsible for this increase in grain size [13].

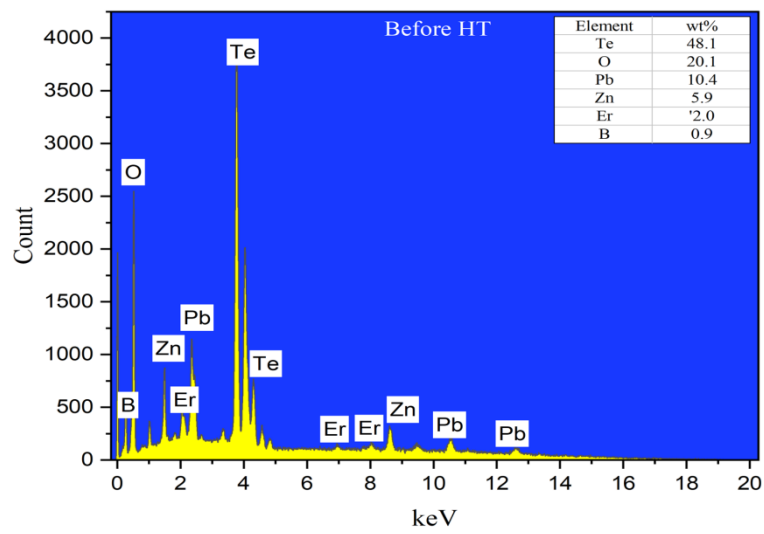


Fig. 3. EDX spectra before heat treatment.

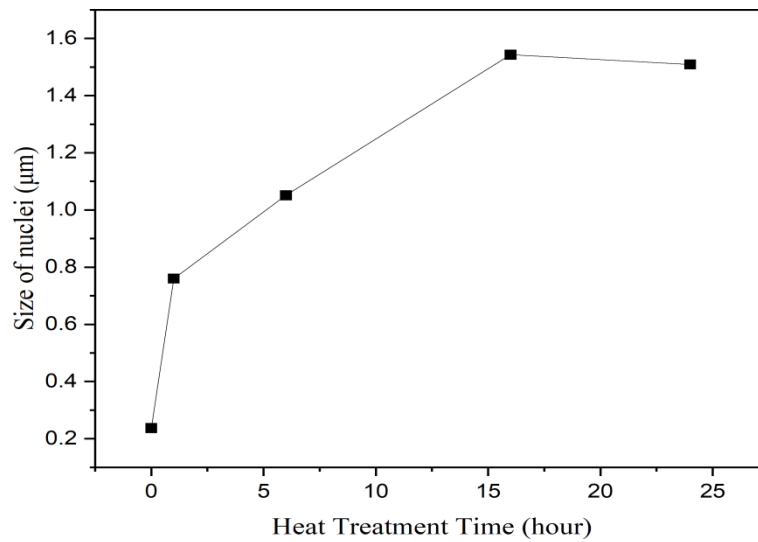


Fig. 4. Size of nuclei as heat treatment time increases.

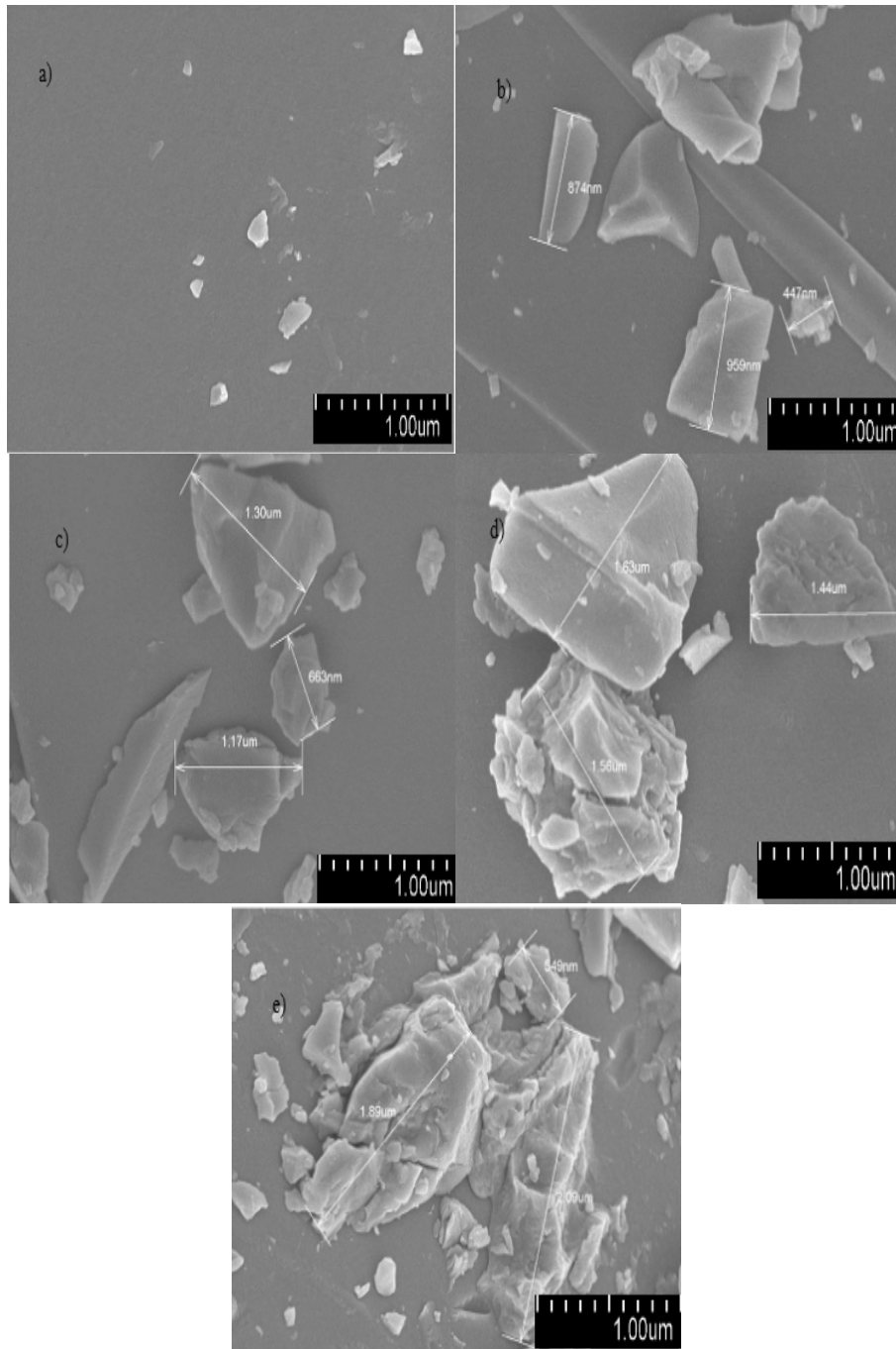


Fig. 5. FESEM micrographs of a) Before HT b) 1h of HT (c) 6h of HT (d) 16h of HT and (e) 24h of HT.

### 3.4 Microwave Dielectric Properties

The dielectric properties were studied using the resonant method at a frequency range around 7 GHz. Figure 6 displays the glass-ceramics' dielectric constants at various crystallization times. Of all the samples, the dielectric constant at 24 hours of heat treatment is clearly the greatest. The dielectric constant shows an initial decrease when heat treatment time is added to 1 hour and then increases, stabilizes and shows a sharp increase when prolonged crystallization time, reaching a maximum dielectric constant value of 18.79 at 24 hours. It is thought that extending the heat treatment period will improve the sample's crystallization and raise the dielectric constant.

As glass undergoes heat treatment, the amorphous glass matrix begins to crystallize and become glass ceramics. Small crystallite initially form and gradually grow into larger grains over time. This crystallization process enhances the material's dielectric properties because crystalline

regions typically have higher dielectric constants than the amorphous glassy phase. Longer heat treatment time allows for the growth and perhaps the stabilization of certain phases that possess higher dielectric constants, thus increasing the overall dielectric constant of the material. The dielectric constant is influenced by the ability of the material to polarize in response to an applied electric field [14]. In crystalline regions, the atomic or ionic arrangements can respond more efficiently to the electric field compared to the disordered amorphous regions. As crystallinity increases with heat treatment time, the enhanced alignment and polarization within the crystalline structure contribute to a higher dielectric constant. The relative volume fraction of grain boundaries decreases, and the contribution of the higher dielectric constant of the grain interiors becomes more significant. However, excessive grain growth can lead to the development of larger grain boundaries or even new interfaces that could act as barriers to polarization, decreasing the dielectric constant [15]. Figure 7 shows the tangent delta values indicating dielectric loss. The loss factor shows decreasing trend from  $2.89 \times 10^{-4}$  at 0 hours to a minimum of  $1.03 \times 10^{-4}$  at 16 hours, indicating reduced dielectric losses as the microstructure become more crystalline and less defective. However, after 24 hours, a slight increase in tangent delta to  $1.53 \times 10^{-4}$  is observed which may be attributed to microstructural defects such as pores or secondary phase formation from excessive crystallization [15].

Table 2. Changes in dielectric constant and dielectric loss.

Sample	Dielectric Constant ( $\epsilon^*$ ) $\pm 9\%$	Tangent delta, $\tan \delta$ ( $10^{-4}$ ) $\pm 17\%$
BTPZE	18.29	2.89
BTPZE-1	17.49	2.29
BTPZE-6	18.16	1.27
BTPZE-16	17.75	1.03
BTPZE-24	18.79	1.53

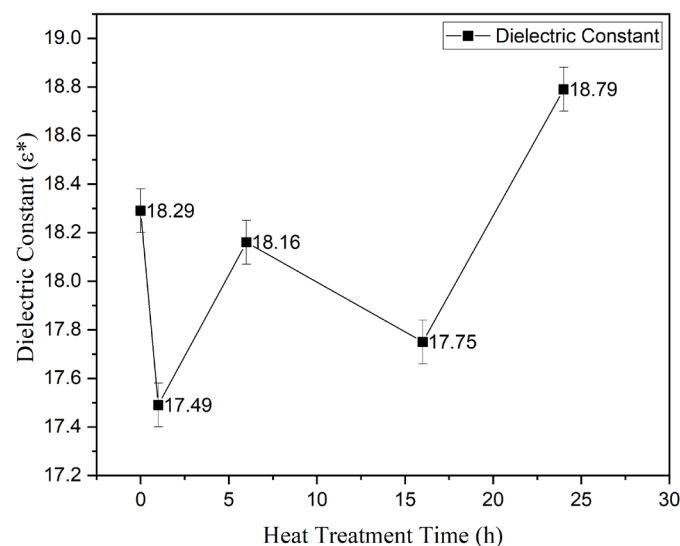


Fig. 6. Variation of dielectric constant ( $\epsilon^*$ ) versus heat treatment time (hours).

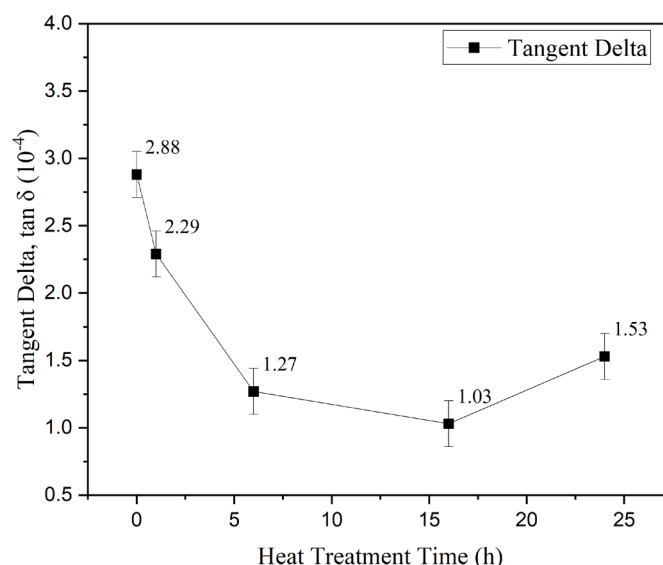


Fig. 7. Variation of dielectric losses ( $\tan \delta$ ) versus heat treatment time (hours).

#### 4. Conclusion

The impact of heat treatment duration on the glass-ceramics' microstructure and dielectric characteristics has been examined. As the crystallization time grew, so did the size and composition of the crystal grains. Simultaneously, a rise in the maximum dielectric constant and reduce of microwave loss were noted. The dielectric constant and dissipation factor of the studies were calculated using the resonant method with a resonant frequency greater than 1 GHz. The dielectric constant increased with crystallization time, reaching its peak after 24 hours of heat treatment. Erbium borotellurite glass ceramics which having a high dielectric constant in the microwave range are crucial for enhancing performance, miniaturization, and efficiency in a wide range of high-frequency applications, including communication devices, sensors, antennas, imaging systems, and energy storage solutions.

#### Acknowledgements

The author acknowledges the Fundamental Research Grant Scheme (FRGS), grant number FRGS/1/2021/STG07/UTM/03/1 funded by the Ministry of Higher Education (MOHE) with matching grant 04M54.

#### References

- [1] C. Devaraja, G. V. J. Gowda, B. Eraiah, A. M. Talwar, A. Dahshan, S. Nazrin, Journal of Alloys and Com- pounds 898 (2022) 162967; <https://doi.org/10.1016/j.jallcom.2021.162967>
- [2] E. Haily, L. Bih, A. El Bouari, A. Lahmar, M. El Marssi, B. Manoun, Journal of the Australian Ceramic Society 56 (4) (2020) 1467-1479; <https://doi.org/10.1007/s41779-020-00473-1>
- [3] A. Malge, T. Sankarappa, T. Sujatha, J. S. Ashwajeet, G. B. Devidas, AIP Conference Proceedings 2161 (1) (2019) 020026; <https://doi.org/10.1063/1.5127617>
- [4] S. Shuhaimi, R. Hisam, A. Yahya, Solid State Sciences 107 (2020) 106345;



<https://doi.org/10.1016/j.solidstatesciences.2020.106345>

- [5] Hrabovský, J., Strážik, L., Désévéday, F., Tazlaru, S., Kučera, M., Nowak, L., Kryštůfek, R., Mistrík, J., Dědič, V., Kopecký, V., Gadret, G., Wágner, T., Smektala, F., Veis, M. (2023). Progress in Materials Science 125 (2022) 100890; <https://doi.org/10.2139/ssrn.4570123>
- [6] P. Naresh, S. A. Priya, P. M. Mohan, B. Kavitha, N. Narsimlu, D. Sreeni-vasu, C. Srinivas, J. L. Naik, K. S. Kumar, AIP Conference Proceedings, Vol. 2162, AIP Publishing LLC, 2019, p. 020007; <https://doi.org/10.1063/1.5130217>
- [7] M. N. Abd Azis, Dielectric behavior in erbium-doped tellurite glass for potential high-energy capacitor (2021).
- [8] E. Sazali, M. Sahar, S. Ghoshal, R. Arifin, M. Rohani, R. Amjad, Journal of Non-Crystalline Solids 410 (2015) 174-179; <https://doi.org/10.1016/j.jnoncrysol.2014.11.036>
- [9] Sebastian, Mailadil, Silva, M. A. S. & Sombra, Sergio. (2017), Measurement of Microwave Dielectric Properties and Factors Affecting Them; <https://doi.org/10.1002/9781119208549.ch1>
- [10] E. Sazali, M. Sahar, S. Ghoshal, R. Arifin, M. Rohani, A. Awang, Journal of Alloys and Compounds 607 (2014) 85-90; <https://doi.org/10.1016/j.jallcom.2014.03.175>
- [11] S. Azmi, M. Sahar, S. K. Ghoshal, R. Arifin, Journal of Non-Crystalline Solids 411 (03-2015); <https://doi.org/10.1016/j.jnoncrysol.2014.12.024>
- [12] T. Sugimoto, Chapter 4 - recrystallization, in: T. Sugimoto (Ed.), Monodispersed Particles (Second Edition), second edition Edition, Elsevier, Amsterdam, 2019, pp. 167-179; <https://doi.org/10.1016/B978-0-444-62749-0.00004-1>
- [13] A. Bouhmouche, A. Jabar, I. Rhrissi, R. Moubah, Materials Science in Semiconductor Processing 175 (2024) 108238; <https://doi.org/10.1016/j.mssp.2024.108238>
- [14] T. Sugimoto, Chapter 4 - recrystallization, in: T. Sugimoto (Ed.), Monodispersed Particles (Second Edition), second edition Edition, Elsevier, Amsterdam, 2019, pp. 167-179; <https://doi.org/10.1016/B978-0-444-62749-0.00004-1>
- [15] S. Duhan, S. Sanghi, A. Agarwal, A. Sheoran, S. Rani, Physica B: Condensed Matter 404 (12-13) (2009) 1648-1; <https://doi.org/10.1016/j.physb.2009.01.041>